$h^0 \to c\bar{c}$ as a test case for quark flavor violation in the MSSM

A. Bartl,[1] H. Eberl,[2] E. Ginina,[2] K. Hidaka,[3,4] and W. Majerotto[2]
[1]*Universität Wien, Fakultät für Physik, A-1090 Vienna, Austria*
[2]*Institut für Hochenergiephysik der Österreichischen Akademie der Wissenschaften, A-1050 Vienna, Austria*
[3]*Department of Physics, Tokyo Gakugei University, Koganei, Tokyo 184-8501, Japan*
[4]*RIKEN Nishina Center for Accelerator-Based Science, Wako, Saitama 351-0198, Japan*
(Received 13 November 2014; published 7 January 2015)

We compute the decay width of $h^0 \to c\bar{c}$ in the minimal supersymmetric Standard Model with quark flavor violation (QFV) at full one-loop level adopting the $\overline{\text{DR}}$ renormalization scheme. We study the effects of $\tilde{c} - \tilde{t}$ mixing, taking into account the constraints from the B meson data. We show that the full one-loop corrected decay width $\Gamma(h^0 \to c\bar{c})$ is very sensitive to the minimal supersymmetric Standard Model QFV parameters. In a scenario with large $\tilde{c}_{L,R} - \tilde{t}_{L,R}$ mixing $\Gamma(h^0 \to c\bar{c})$ can differ up to $\sim \pm 35\%$ from its Standard Model value. After estimating the uncertainties of the width, we conclude that an observation of these supersymmetry QFV effects is possible at an e^+e^- collider (International Linear Collider).

DOI: 10.1103/PhysRevD.91.015007 PACS numbers: 14.80.Da, 11.30.Hv, 14.80.Ly, 12.60.Jv

I. INTRODUCTION

The properties of the Higgs boson, discovered at the LHC, CERN, with a mass of 125.15 ± 0.24 GeV (averaged over the values given by ATLAS [1,2] and CMS [3,4]) [5], are consistent with the prediction of the Standard Model (SM) [6]. Future experiments at the LHC at higher energy ($\sqrt{s} = 14$ TeV) and higher luminosity will provide more precise data on Higgs boson observables, as Higgs production cross sections, decay branching ratios, etc. Even more precise data can be expected at a future e^+e^- linear collider (ILC). This will allow one to test the SM more accurately and will give information on physics beyond the SM. The discovered Higgs boson could also be the lightest neutral Higgs boson h^0 of the minimal supersymmetric Standard Model (MSSM) [6,7].

The decays of h^0 are usually assumed to be quark flavor conserving (QFC). However, quark flavor violation (QFV) in the squark sector may significantly influence the decay widths of h^0 at one-loop level. In particular, the rate of the h^0 decay into a charm-quark pair, $h^0 \to c\bar{c}$, may be significantly different from the SM prediction due to squark generation mixing, especially that between the second and the third squark generations ($\tilde{c}_{L,R} - \tilde{t}_{L,R}$ mixing). This possibility will be studied in detail in the present paper.

It is well known that the mixing between the first and the second squark generations is strongly suppressed by the data on K physics [8]. Therefore, we assume mixing between the second and the third squark generations, respecting the constraints from B physics. In the MSSM this mixing was theoretically studied for squark and gluino production and decays at the LHC [9–17].

The outline of the paper is as follows. In Sec. II we shortly give the definitions of the QFV squark mixing parameters. In Sec. III we present the calculation of the width of $h^0 \to c\bar{c}$ at full one-loop level in the $\overline{\text{DR}}$ renormalization scheme with quark flavor violation within the MSSM. In particular, we give formulas for the important one-loop gluino contribution. In Sec. IV we present a detailed numerical analysis. In Sec. V we study the feasibility of observing the supersymmetry (SUSY) QFV effects in the decay $h^0 \to c\bar{c}$ at the ILC by estimating the theoretical uncertainties. Section VI contains our conclusions.

II. DEFINITION OF THE QFV PARAMETERS

In the MSSM's super-CKM basis of $\tilde{q}_{0\gamma} = (\tilde{q}_{1\text{L}}, \tilde{q}_{2\text{L}}, \tilde{q}_{3\text{L}}, \tilde{q}_{1\text{R}}, \tilde{q}_{2\text{R}}, \tilde{q}_{3\text{R}})$, $\gamma = 1, \ldots 6$, with $(q_1, q_2, q_3) = (u, c, t)$, (d, s, b), one can write the squark mass matrices in their most general 3×3-block form [18],

$$\mathcal{M}^2_{\tilde{q}} = \begin{pmatrix} \mathcal{M}^2_{\tilde{q},LL} & \mathcal{M}^2_{\tilde{q},LR} \\ \mathcal{M}^2_{\tilde{q},RL} & \mathcal{M}^2_{\tilde{q},RR} \end{pmatrix}, \tag{1}$$

with $\tilde{q} = \tilde{u}, \tilde{d}$. The left-left and right-right blocks in Eq. (1) are given by

$$\begin{aligned} \mathcal{M}^2_{\tilde{u},LL} &= V_{\text{CKM}} M^2_Q V^\dagger_{\text{CKM}} + D_{\tilde{u},LL}\mathbf{1} + \hat{m}^2_u, \\ \mathcal{M}^2_{\tilde{u},RR} &= M^2_U + D_{\tilde{u},RR}\mathbf{1} + \hat{m}^2_u, \\ \mathcal{M}^2_{\tilde{d},LL} &= M^2_Q + D_{\tilde{d},LL}\mathbf{1} + \hat{m}^2_d, \\ \mathcal{M}^2_{\tilde{d},RR} &= M^2_D + D_{\tilde{d},RR}\mathbf{1} + \hat{m}^2_d, \end{aligned} \tag{2}$$

where $M_{Q,U,D}$ are the Hermitian soft SUSY-breaking mass matrices of the squarks and $\hat{m}_{u,d}$ are the diagonal mass matrices of the up-type and down-type quarks. Furthermore, $D_{\tilde{q},LL} = \cos 2\beta m^2_Z (T^q_3 - e_q \sin^2\theta_W)$ and $D_{\tilde{q},RR} = e_q \sin^2\theta_W \times \cos 2\beta m^2_Z$, where T^q_3 and e_q are the isospin and electric charge of the quarks (squarks), respectively, and θ_W is the

weak mixing angle. Due to the $SU(2)_L$ symmetry, the left-left blocks of the up-type and down-type squarks in Eq. (2) are related by the Cabibbo-Kobayashi-Maskawa (CKM) matrix V_{CKM}. The left-right and right-left blocks of Eq. (1) are given by

$$\mathcal{M}^2_{\tilde{u},RL} = \mathcal{M}^{2\dagger}_{\tilde{u},LR} = \frac{v_2}{\sqrt{2}} T_U - \mu^* \hat{m}_u \cot\beta,$$
$$\mathcal{M}^2_{\tilde{d},RL} = \mathcal{M}^{2\dagger}_{\tilde{d},LR} = \frac{v_1}{\sqrt{2}} T_D - \mu^* \hat{m}_d \tan\beta, \quad (3)$$

where $T_{U,D}$ are the soft SUSY-breaking trilinear coupling matrices of the up-type and down-type squarks entering the Lagrangian $\mathcal{L}_{\rm int} \supset -(T_{U\alpha\beta}\tilde{u}^\dagger_{R\alpha}\tilde{u}_{L\beta}H^0_2 + T_{D\alpha\beta}\tilde{d}^\dagger_{R\alpha}\tilde{d}_{L\beta}H^0_1)$, μ is the Higgsino mass parameter, and $\tan\beta$ is the ratio of the vacuum expectation values of the neutral Higgs fields v_2/v_1, with $v_{1,2} = \sqrt{2}\langle H^0_{1,2}\rangle$. The squark mass matrices are diagonalized by the 6×6 unitary matrices $U^{\tilde{q}}$, $\tilde{q} = \tilde{u}, \tilde{d}$, such that

$$U^{\tilde{q}} \mathcal{M}^2_{\tilde{q}} (U^{\tilde{q}})^\dagger = \mathrm{diag}(m^2_{\tilde{q}_1}, \ldots, m^2_{\tilde{q}_6}), \quad (4)$$

with $m_{\tilde{q}_1} < \cdots < m_{\tilde{q}_6}$. The physical mass eigenstates $\tilde{q}_i$, $i = 1, \ldots, 6$ are given by $\tilde{q}_i = U^{\tilde{q}}_{i\alpha}\tilde{q}_{0\alpha}$.

We define the QFV parameters in the up-type squark sector $\delta^{LL}_{\alpha\beta}$, $\delta^{uRR}_{\alpha\beta}$ and $\delta^{uRL}_{\alpha\beta}$ $(\alpha \neq \beta)$ as [19]

$$\delta^{LL}_{\alpha\beta} \equiv M^2_{Q\alpha\beta} / \sqrt{M^2_{Q\alpha\alpha} M^2_{Q\beta\beta}}, \quad (5)$$

$$\delta^{uRR}_{\alpha\beta} \equiv M^2_{U\alpha\beta} / \sqrt{M^2_{U\alpha\alpha} M^2_{U\beta\beta}}, \quad (6)$$

$$\delta^{uRL}_{\alpha\beta} \equiv (v_2/\sqrt{2}) T_{U\alpha\beta} / \sqrt{M^2_{U\alpha\alpha} M^2_{Q\beta\beta}}, \quad (7)$$

where $\alpha, \beta = 1, 2, 3$ $(\alpha \neq \beta)$ denote the quark flavors u, c, t. In this study we consider $\tilde{c}_R - \tilde{t}_L$, $\tilde{c}_L - \tilde{t}_R$, $\tilde{c}_R - \tilde{t}_R$, and $\tilde{c}_L - \tilde{t}_L$ mixing which is described by the QFV parameters δ^{uRL}_{23}, $\delta^{uLR}_{23} \equiv (\delta^{uRL}_{32})^*$, δ^{uRR}_{23}, and δ^{LL}_{23}, respectively. We also consider $\tilde{t}_L - \tilde{t}_R$ mixing described by the QFC parameter δ^{uRL}_{33} which is defined by Eq. (7) with $\alpha = \beta = 3$. All QFV parameters and δ^{uRL}_{33} are assumed to be real.

III. $h^0 \to c\bar{c}$ AT FULL ONE-LOOP LEVEL WITH FLAVOR VIOLATION

We study the decay of the lightest neutral Higgs boson, h^0, into a pair of charm quarks (Fig. 1) at full one-loop level in the general MSSM with quark flavor violation in the squark sector. The full one-loop decay width of $h^0 \to c\bar{c}$ was first calculated within the QFC MSSM by Ref. [20]. In [21–23] higher order SUSY corrections for the Higgs-fermion-fermion vertices were calculated in the generic MSSM in an effective-field-theory approach.

The decay width of the reaction $h^0 \to c\bar{c}$ including one-loop contributions can be written as

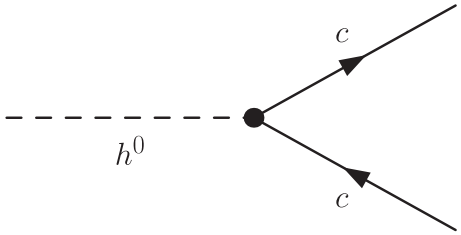

FIG. 1. h^0 decay into a pair of charm quarks.

$$\Gamma(h^0 \to c\bar{c}) = \Gamma^{\rm tree}(h^0 \to c\bar{c}) + \delta\Gamma^{\rm 1loop}(h^0 \to c\bar{c}). \quad (8)$$

The tree-level decay width $\Gamma^{\rm tree}(h^0 \to c\bar{c})$ reads

$$\Gamma^{\rm tree}(h^0 \to c\bar{c}) = \frac{N_C}{8\pi} m_{h^0} (s^c_1)^2 \left(1 - \frac{4m^2_c}{m^2_{h^0}}\right)^{3/2}, \quad \text{with} \quad N_C = 3, \quad (9)$$

where m_{h^0} is the on-shell (OS) mass of h^0 and the tree-level coupling s^c_1 is

$$s^c_1 = -g\frac{m_c}{2m_W}\frac{\cos\alpha}{\sin\beta} = -\frac{h_c}{\sqrt{2}}\cos\alpha. \quad (10)$$

Here α is the mixing angle of the two CP-even Higgs bosons, h^0 and H^0 [24].

In the general MSSM at one-loop level, in addition to the diagrams that contribute within the SM, $\delta\Gamma^{\rm 1loop}(h^0 \to c\bar{c})$ also receives contributions from diagrams with additional Higgs bosons and supersymmetric particles. The contributions from SUSY particles are shown in Fig. 2, neglecting the contributions from scalar leptons. The flavor violation is induced by one-loop diagrams with squarks that have a mixed quark flavor nature. In addition, the coupling of h^0 with two squarks $\tilde{u}_i\tilde{u}_j$ [see Eq. (A3) of Appendix A] contains the trilinear coupling matrices $(T_U)_{ij}$ which for $i \neq j$ break quark flavor explicitly.

The one-loop contributions to $\Gamma(h^0 \to c\bar{c})$ contain three parts, QCD (g) corrections, SUSY-QCD $(\tilde{g})$ corrections, and electroweak (EW) corrections. In the latter we also include the Higgs contributions. In the following we will mainly give details for the QCD and SUSY-QCD corrections.

A. Renormalization procedure

Loop calculations can lead to an UV- and IR-divergent result and therefore require renormalization. To get an UV finite result, we adopt in our study the $\overline{\rm DR}$ renormalization scheme, where all input parameters in the tree-level Lagrangian (masses, fields, and coupling parameters) are UV finite, defined at the scale $Q = 125.5$ GeV $\simeq m_{h^0}$, and the UV divergence parameter $\Delta = \frac{2}{\epsilon} - \gamma + \ln 4\pi$, where $\epsilon = 4 - D$ in a D-dimemsional space-time and γ is the Euler–Mascheroni constant, is set to zero. The tree-level coupling is defined at the given scale and thus does not receive further finite shifts due to loop corrections. To obtain

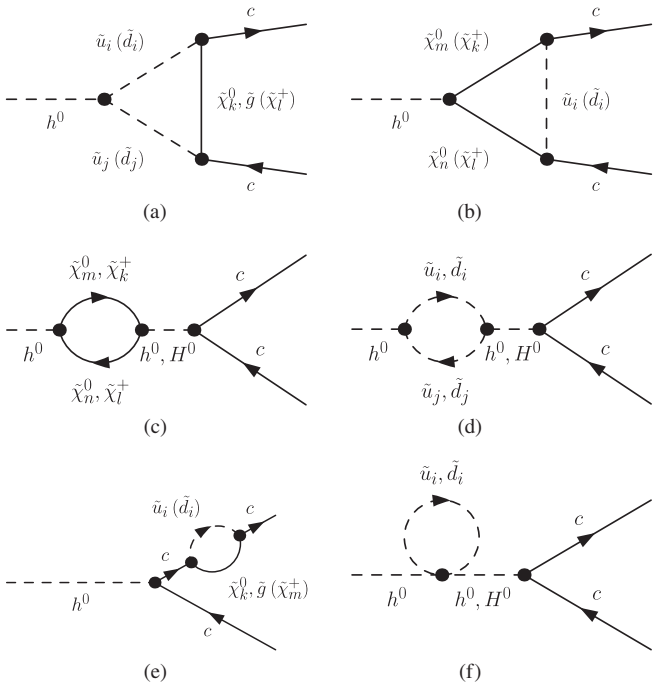

FIG. 2. The main one-loop contributions with SUSY particles in $h^0 \to c\bar{c}$. The corresponding diagram to (e) with the self-energy contribution to the other charm quark is not shown explicitly.

the shifts from the $\overline{\rm DR}$ masses and fields to the physical scale-independent masses and fields, we use on-shell renormalization conditions. To ensure IR convergence, we include in our calculations the contribution of the real hard gluon/photon radiation from the final charm quarks assuming a small gluon/photon mass λ.

The one-loop corrected width of the process $h^0 \to c\bar{c}$ including hard gluon/photon radiation is given by

$$\Gamma(h^0 \to c\bar{c}) = \Gamma^{\rm tree}(h^0 \to c\bar{c}) + \sum_{x=g,\tilde{g},{\rm EW}} \delta\Gamma^x, \qquad (11)$$

where $\delta\Gamma^x$ read

$$\delta\Gamma^{\tilde{g}} = \frac{3}{4\pi} m_{h^0} s_1^c {\rm Re}(\delta S_1^{c,\tilde{g}}) \left(1 - \frac{4m_c^2}{m_{h^0}^2}\right)^{3/2}, \qquad (12)$$

$$\delta\Gamma^{g/{\rm EW}} = \frac{3}{4\pi} m_{h^0} s_1^c {\rm Re}(\delta S_1^{c,g/{\rm EW}}) \left(1 - \frac{4m_c^2}{m_{h^0}^2}\right)^{3/2} + \Gamma^{\rm hard}(h^0 \to c\bar{c}g/\gamma). \qquad (13)$$

Note that all parameters in the tree-level coupling s_1^c, Eq. (10), are $\overline{\rm DR}$ running at the scale Q = 125.5 GeV. The renormalized finite one-loop amplitude of the process is a sum of all vertex diagrams, the amplitudes arising from the wave-function renormalization constants and the amplitudes arising from the coupling counterterms. Note that in the $\overline{\rm DR}$ renormalization scheme the counterterms contain only UV-divergent parts and have to cancel in order to yield a convergent result. The one-loop renormalized coupling correction can be written as

$$\delta S_1^{c,x} = \delta S_1^{c,x(v)} + \delta S_1^{c,x(w)} + \delta S_1^{c,x(0)}, \qquad x = g, \tilde{g}, {\rm EW}, \qquad (14)$$

where $\delta S_1^{c,x(v)}$ is the vertex coupling correction, $\delta S_1^{c,x(w)}$ is the wave-function coupling correction, and $\delta S_1^{c,x(0)}$ is the coupling counterterm. The tree-level interaction Lagrangian of the lightest Higgs boson h^0 and two charm quarks is given by Eq. (A1) in Appendix A. The renormalized Lagrangian $\mathcal{L}^{\rm ren}$ is obtained after making the replacement $\mathcal{L}^{\overline{\rm DR}} = \mathcal{L}^{\rm ren} + \delta\mathcal{L}$, where $\delta\mathcal{L} = -\delta S_1^{c(v)} h^0 \bar{c} c$ describes all vertex-type interactions. The coupling correction due to wave-function renormalization is given by

$$\delta S_1^{c(w)} = \frac{s_1^c}{2}\delta Z_{h^0} + \frac{s_2^c}{2}\delta Z_{h^0 H^0} + \frac{s_1^c}{4}(\delta Z_c^L + \delta Z_c^{L*} + \delta Z_c^R + \delta Z_c^{R*}), \qquad (15)$$

where s_2^c is the coupling of the heavier neutral Higgs H^0 and the charm quark, $s_2^c = -\frac{h_c}{\sqrt{2}}\sin\alpha$. The charm quark wave-function renormalization constants read

$$\begin{aligned}\delta Z_c^{L/R} = &-\widetilde{\rm Re}\Pi_{cc}^{L/R}(m_c) + \frac{1}{2m_c}\widetilde{\rm Re}(\Pi_{cc}^{S,L/R}(m_c) - \Pi_{cc}^{S,R/L}(m_c)) \\ &- m_c \widetilde{\rm Re}[m_c(\dot{\Pi}_{cc}^{L/R}(m_c) + \dot{\Pi}_{cc}^{R/L}(m_c)) \\ &+ \dot{\Pi}_{cc}^{S,L/R}(m_c) + \dot{\Pi}_{cc}^{S,R/L}(m_c)], \end{aligned} \qquad (16)$$

and the Higgs wave-function renormalization constants for the case of $h^0 - H^0$ mixing are given by

$$\delta Z_{h^0} = -\widetilde{\rm Re}\dot{\Pi}_{h^0 h^0}(m_{h^0}^2), \qquad (17)$$

$$\delta Z_{h^0 H^0} = \frac{2}{m_{h^0}^2 - m_{H^0}^2}(\widetilde{\rm Re}\Pi_{h^0 H^0}(m_{h^0}^2) - \delta t_{h^0 H^0}), \qquad (18)$$

with the tadpole contribution

$$\delta t_{h^0 H^0} = -\frac{1}{v}\left[\tau_{h^0}\left(\frac{s_\alpha^2 c_\alpha}{c_\beta} + \frac{c_\alpha^2 s_\alpha}{s_\beta}\right) + \tau_{H^0}\left(-\frac{c_\alpha^2 s_\alpha}{c_\beta} + \frac{s_\alpha^2 c_\alpha}{s_\beta}\right)\right], \qquad (19)$$

where $c_\alpha = \cos\alpha$ and $s_\alpha = \sin\alpha$. τ_{h^0} and τ_{H^0} are the loop corrections from the tadpole diagrams with h^0 and H^0, respectively. In Eqs. (16), (17), and (18), $\widetilde{\rm Re}$ applied to the self-energies denoted by Π takes the real part of the loop integrals but leaves the possible complex couplings

unaffected. Finally, the coupling counterterm $\delta S_1^{c(0)}$ is given by

$$\frac{\delta S_1^{c(0)}}{s_1^c} = \left(\frac{\delta g}{g} + \frac{\delta m_c}{m_c} - \frac{\delta m_W}{m_W} - \frac{\delta \sin\beta}{\sin\beta} + \frac{\delta \cos\alpha}{\cos\alpha}\right)_\Delta, \quad (20)$$

where the subindex Δ means that only the part proportional to the UV divergence parameter Δ is taken. The explicit expressions for the shifts of the parameters in (20) can be found in Ref. [25]. Note that $\frac{\delta g}{g} = \frac{\delta e}{e} - \frac{\delta \sin\theta_W}{\sin\theta_W}$ is used.

B. One-loop gluon contribution

The one-loop virtual gluon contribution to $\Gamma(h^0 \to c\bar{c})$ is given by

$$\delta\Gamma^g = \frac{3}{4\pi} m_{h^0} s_1^c \mathrm{Re}(\delta S_1^{c,g}) \beta^3, \quad (21)$$

with $\beta = (1 - 4m_c^2/m_{h^0}^2)^{1/2}$. $\delta S_1^{c,g}$ contains terms originating from the vertex correction, the wave-function correction, and the coupling correction due to gluon interaction,

$$\delta S_1^{c,g} = \delta S_1^{c(g,v)} + \delta S_1^{c(g,w)} + \delta S_1^{c(g,0)}. \quad (22)$$

The individual contributions in $\delta S_1^{c,g}$ are given by

$$\delta S_1^{c(g,v)} = \frac{2\alpha_s}{3\pi} s_1^c [2B_0 - r - (m_{h^0}^2 - 2m_c^2) C_0 - 4m_c^2 C_1], \quad (23)$$

$$\delta S_1^{c(g,w)} = \frac{2\alpha_s}{3\pi} s_1^c \left[-B_0 - B_1 + \frac{r}{2} + 2m_c^2(\dot{B}_0 - \dot{B}_1)\right], \quad (24)$$

$$\delta S_1^{c(g,0)} = \frac{2\alpha_s}{3\pi} s_1^c \left(B_1 - B_0 + \frac{r}{2}\right), \quad (25)$$

where $r = 0$ in the $\overline{\mathrm{DR}}$ scheme and $r = 1$ in the $\overline{\mathrm{MS}}$ scheme. $B_k, \dot{B}_k$, and C_k are the two- and three-point functions

$$B_k = B_k(m_c^2, 0, m_c^2), \quad (26)$$

$$\dot{B}_k = \left.\frac{\partial B_k(p^2, \lambda^2, m_c^2)}{\partial p^2}\right|_{p^2 = m_c^2}, \quad (27)$$

$$C_k = C_k(m_c^2, m_{h^0}^2, m_c^2, \lambda^2, m_c^2, m_c^2), \quad (28)$$

with $k = 0, 1$. Summing up Eqs. (23)–(25), one can write $\delta S_1^{c,g}$ in the form

$$\delta S_1^{c,g} = \frac{2}{3}\frac{\alpha_s}{\pi} s_1^c \Delta^{\mathrm{H,virt}}(\beta). \quad (29)$$

Furthermore, we will use the result for the hard gluon radiation, given in Appendix B. We can write Eq. (B2) in the form

$$\Gamma^{\mathrm{hard}}(h^0 \to c\bar{c}g) = \frac{3}{8\pi} m_{h^0} (s_1^c)^2 \beta^3 \frac{4}{3}\frac{\alpha_s}{\pi} \Delta^{\mathrm{H,hard}}(\beta). \quad (30)$$

Combining (21), (29), and (30) for the gluon one-loop corrected convergent width, we obtain

$$\Gamma^g(h^0 \to c\bar{c}) = \Gamma^{\mathrm{tree}} + \delta\Gamma^g + \Gamma^{g,\mathrm{hard}} = \frac{3}{8\pi} m_{h^0} (s_1^c)^2 \beta^3 \left(1 + \frac{4}{3}\frac{\alpha_s}{\pi}\Delta^{\mathrm{H}}(\beta)\right), \quad (31)$$

where $\Delta^{\mathrm{H}}(\beta) = \Delta^{\mathrm{H,virt}}(\beta) + \Delta^{\mathrm{H,hard}}(\beta)$ is the result of Ref. [26] and its explicit expression can be found therein or e.g. in Refs. [20,27,28]. Equation (31) can be written in a compact form as

$$\Gamma^g(h^0 \to c\bar{c}) = \Gamma^{\mathrm{tree}}(m_c|_{\mathrm{OS}}) \left(1 + \frac{4}{3}\frac{\alpha_s}{\pi}\Delta^{\mathrm{H}}(\beta)\right), \quad (32)$$

where $m_c|_{\mathrm{OS}}$ denotes the OS charm quark mass. Note that the result for the photon one-loop corrected convergent width is obtained from (32) by making the replacement $\frac{4}{3}\alpha_s \to e_c^2\alpha$:

$$\Gamma^\gamma(h^0 \to c\bar{c}) = \Gamma^{\mathrm{tree}}(m_c|_{\mathrm{OS}}) \left(1 + \frac{4}{9}\frac{\alpha}{\pi}\Delta^{H}(\beta)\right), \quad (33)$$

with $\alpha = e^2/(4\pi)$.

For $m_c \ll m_{h^0}$ $(\beta \to 1)$

$$\Delta^{\mathrm{H}} = -3\ln\frac{m_{h^0}}{m_c|_{\mathrm{OS}}} + \frac{9}{4}, \quad (34)$$

and from Eq. (25) using Eqs. (C7) and (C8), we get

$$\frac{\delta m_c^g}{m_c} = \frac{\delta S_1^{c,(g,0)}}{s_1^c} = \frac{\alpha_s}{3\pi}\left(-6\ln\frac{m_{h^0}}{m_c|_{\mathrm{OS}}} + r - 5\right). \quad (35)$$

For $\Gamma^g(h^0 \to c\bar{c})$ in the limit $m_c \ll m_{h^0}$, we obtain

$$\Gamma^g(h^0 \to c\bar{c}) = \Gamma^{\mathrm{tree}}(m_c|_{\mathrm{SM}}) \left(1 + \frac{19 - 2r}{3}\frac{\alpha_s}{\pi}\right), \quad (36)$$

where in (36) we have absorbed the logarithm of δm_c^g into

$$m_c|_{\mathrm{SM}} = m_c|_{\mathrm{OS}} + \delta m_c^g. \quad (37)$$

Combining Eq. (35) with Eqs. (36) and (37), one can see that the one-loop level $\Gamma^g(h^0 \to c\bar{c})$ does not depend on the parameter r. In the numerical evaluation of $m_c|_{\mathrm{SM}}$, we follow the recipe given in Ref. [29], starting with Eq. (4), and we use $\alpha_s^{(2)}(\mathrm{Q})$ given therein. In all other cases, we take $\alpha_s(\mathrm{Q})$ from SPheno [30,31], where it is calculated at two-loop level within the MSSM. To stay consistent, in our numerical calculations, we have included in addition only the gluonic α_s^2 contributions, taken from Ref. [28].

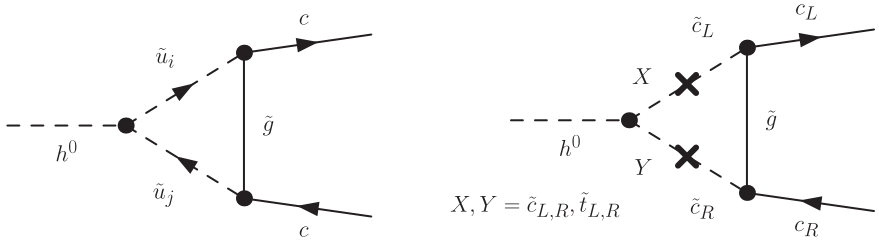

FIG. 3. (a) Gluino vertex contribution to $h^0 \to c\bar{c}$ and (b) examples of quark flavor mixing in the gluino vertex contribution.

With these, $\Gamma^g(h^0 \to c\bar{c})$ will be denoted as $\Gamma^{g,\mathrm{impr}}(h^0 \to c\bar{c})$,

$$\Gamma^{g,\mathrm{impr}}(h^0 \to c\bar{c}) = \Gamma^{\mathrm{tree}}(m_c|_{\mathrm{SM}}) + \delta\Gamma^g(m_c|_{\mathrm{SM}}). \quad (38)$$

C. One-loop gluino contribution and decoupling limit

The one-loop gluino contribution to $\Gamma(h^0 \to c\bar{c})$, Figs. 3 and 4, renormalized in the $\overline{\mathrm{DR}}$ scheme reads

$$\delta\Gamma^{\tilde{g}} = \frac{3}{4\pi} m_{h^0} s_1^c \mathrm{Re}(\delta S_1^{c,\tilde{g}})\beta^3. \quad (39)$$

$\delta S_1^{c,\tilde{g}}$ acquires contributions from the vertex correction (Fig. 3), the wave-function correction (Fig. 4), and the coupling correction due to gluino interaction,

$$\delta S_1^{c,\tilde{g}} = \delta S_1^{c(\tilde{g},v)} + \delta S_1^{c(\tilde{g},w)} + \delta S_1^{c(\tilde{g},0)}. \quad (40)$$

In the following we will use the abbreviations $\alpha_{ij} = U^{\tilde{u}*}_{i2} U^{\tilde{u}}_{j2} + U^{\tilde{u}*}_{i5} U^{\tilde{u}}_{j5}$ and $\beta_{ij} = U^{\tilde{u}*}_{i2} U^{\tilde{u}}_{j5} + U^{\tilde{u}*}_{i5} U^{\tilde{u}}_{j2}$. Note that applying Einstein sum convention we get $\alpha_{ii} = 2$ and $\beta_{ii} = 0$. Neglecting the charm quark mass and the Higgs boson mass compared to the squark and gluino masses, one can write the individual contributions as

$$\delta S_1^{c(\tilde{g},v)} = \frac{\alpha_s}{3\pi} \sum_{i,j=1}^{6} G^{\tilde{u}}_{ij1} m_{\tilde{g}} \beta_{ij} C_0^{ij}, \quad (41)$$

$$\delta S_1^{c(\tilde{g},w)} = \frac{\alpha_s}{3\pi} s_1^c \sum_{i=1}^{6} (\alpha_{ii} B_1^i + 4 m_{\tilde{g}} \beta_{ii} \dot{B}_0^i), \quad (42)$$

where the coupling $G^{\tilde{u}}_{ij1}$ is given in Eq. (A3) of Appendix A. For the following discussion of the gluino contribution in the large $m_{\tilde{g}}$ limit, we give the charm mass counterterm $\delta m_c^{\tilde{g}}$ in the OS scheme, which has an UV-divergent and a finite contribution,

$$\delta m_c^{\tilde{g}} = -\frac{\alpha_s}{3\pi} \sum_{i=1}^{6} (m_c \alpha_{ii} B_1^i + m_{\tilde{g}} \beta_{ii} B_0^i). \quad (43)$$

For the gluino contribution, we have $\delta S_1^{c(\tilde{g},0)}/s_1^c = \delta m_c^{\tilde{g}}/m_c$. Therefore, with Eq. (42) we get

$$\delta S_1^{c(\tilde{g},0)} = -\frac{\alpha_s}{3\pi} s_1^c \sum_{i=1}^{6} \left(\alpha_{ii} B_1^i + \frac{m_{\tilde{g}}}{m_c} \beta_{ii} B_0^i \right). \quad (44)$$

In the $\overline{\mathrm{DR}}$ scheme, we need only the UV-divergent part of (44) which is

$$\delta S_1^{c(\tilde{g},0)} = 6 \frac{\alpha_s}{3\pi} s_1^c \Delta. \quad (45)$$

Δ is the UV divergence factor. In Eqs. (41)–(44) $B_k^i, \dot{B}_0^i$, and C_0^i are the two- and three-point functions

$$B_k^i = B_k(0, m_{\tilde{g}}^2, m_{\tilde{u}_i}^2), \quad k = 0, 1, \quad i = 1, \ldots, 6, \quad (46)$$

$$\dot{B}_0^i = \left. \frac{\partial B_0(p^2, m_{\tilde{g}}^2, m_{\tilde{u}_i}^2)}{\partial p^2} \right|_{p^2=0}, \quad i = 1, \ldots, 6, \quad (47)$$

$$C_0^{ij} = C_k(0, 0, 0, m_{\tilde{g}}^2, m_{\tilde{u}_i}^2, m_{\tilde{u}_j}^2), \quad i = 1, \ldots, 6. \quad (48)$$

The total correction $\delta S_1^{c,\tilde{g}}$ [Eq. (40)] is given by

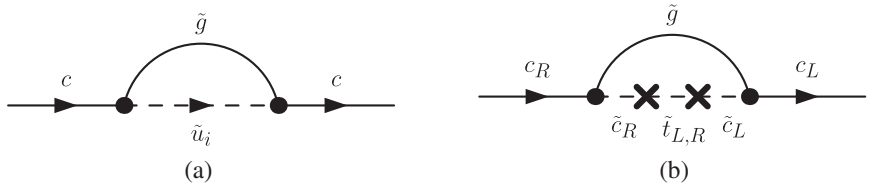

FIG. 4. (a) The gluino contribution to the charm quark self-energy and (b) examples of quark flavor mixing in the charm quark self-energy contribution with gluino.

$$\overline{\text{DR}}\text{ scheme: } \delta S_1^{c,\tilde{g}} = \frac{\alpha_s}{3\pi}\sum_{i,j=1}^{6}\{m_{\tilde{g}}\beta_{ij}(G^{\tilde{u}}_{ij1}C_0^{ij} + 4s_1^c\delta_{ij}\dot{B}_0^i) + s_1^c\delta_{ij}(\alpha_{ii}B_1^i + \Delta)\} \tag{49}$$

$$\text{OS scheme: } \delta S_1^{c,\tilde{g}} = \frac{\alpha_s}{3\pi}\sum_{i,j=1}^{6}\left\{m_{\tilde{g}}\beta_{ij}(G^{\tilde{u}}_{ij1}C_0^{ij} + 4s_1^c\delta_{ij}\dot{B}_0^i) - s_1^c\delta_{ij}\frac{m_{\tilde{g}}}{m_c}\beta_{ii}B_0^i\right\}. \tag{50}$$

As $B_1^i \to -\Delta/2$ and thus $\alpha_{ii}B_1^i \to -\Delta$, (49) is UV convergent. As $\beta_{ii}B_0^i \to 0$, also (50) is UV convergent.

In the limit $m_{\tilde{g}} \to \infty$, from (C19) it follows $m_{\tilde{g}}C_0^{ij} \to 0$, and from (C12) it follows $\dot{B}_0^i \to 0$. However, in this limit (C3) and (C4) become independent of the index i and grow with $\ln\frac{m_{\tilde{g}}^2}{m_{h^0}^2}$. Therefore, $\beta_{ii}B_0^i \to 0$ guarantees decoupling of the gluino loop contribution in the OS scheme.

In the $\overline{\text{DR}}$ scheme for $m_{\tilde{g}} \to \infty$, we get

$$\delta S_1^{c,\tilde{g}} \sim \frac{2\alpha_s}{3\pi}s_1^c B_1^i \quad \text{with} \quad B_1 \sim \ln\frac{m_{\tilde{g}}^2}{m_{h^0}^2}. \tag{51}$$

At first sight it seems that the gluino contribution does not decouple for $m_{\tilde{g}} \to \infty$. However, the tree-level coupling s_1^c [Eq. (10)] contains a factor m_c. We have

$$m_c(m_{h^0})|_{\overline{\text{DR}}} = m_c(m_c)|_{\overline{\text{MS}}} + \delta m_c^{\tilde{g}} + \ldots, \tag{52}$$

where we take $m_c(m_c)|_{\overline{\text{MS}}} = 1.275$ GeV as input [32]. $\delta m_c^{\tilde{g}}$ is due to the self-energy contributions with gluino [see Figs. 4(a) and 4(b)]. We get

$$\delta m_c^{\tilde{g}} \sim -\frac{2\alpha_s}{3\pi}m_c B_1^i. \tag{53}$$

Thus, the sum $\Gamma^{\text{tree}} + \delta\Gamma^{\tilde{g}}$ is indeed decoupling for $m_{\tilde{g}} \to \infty$. Analogously, this also holds for the chargino and neutralino contributions.

D. Total result for the width at full one-loop level

Finally, we want to sum up all contributions to get the total result for $\Gamma(h^0 \to c\bar{c})$ at full one-loop level.

The one-loop result including gluino and EW contributions reads

$$\Gamma^{\tilde{g}+\text{EW}}(h^0 \to c\bar{c}) = \Gamma^{\text{tree}}(m_c) + \delta\Gamma^{\tilde{g}}(m_c) + \delta\Gamma^{\text{EW}}(m_c), \tag{54}$$

where Γ^{tree}, $\delta\Gamma^{\tilde{g}}$, and $\delta\Gamma^{\text{EW}}$ are given by Eqs. (9), (39), and (13), respectively. Note that Eq. (54) is a series expansion around $\Gamma^{\text{tree}}(m_c) = \Gamma^{\text{tree}}(m_c(m_{h^0})|_{\overline{\text{DR}}})$. However, the improved result with gluon contribution [Eq. (38)] given by

$$\Gamma(h^0 \to c\bar{c})^{g,\text{impr}} = \Gamma^{\text{tree}}(m_c|_{\text{SM}}) + \delta\Gamma^{g}(m_c|_{\text{SM}}) \tag{55}$$

is a series expansion around $\Gamma^{\text{tree}}(m_c|_{\text{SM}})$. to combine Eqs. (54) and (55) in a consistent way, we write

$$\Gamma^{\text{tree}}(m_c|_{\text{SM}}) = \Gamma^{\text{tree}}(m_c)\frac{m_c^2|_{\text{SM}}}{m_c^2}, \tag{56}$$

and therefore

$$\Gamma^{\text{tree}}(m_c|_{\text{SM}}) = \Gamma^{\text{tree}}(m_c) - \Gamma^{\text{tree}}(m_c)\frac{m_c^2 - m_c^2|_{\text{SM}}}{m_c^2}. \tag{57}$$

TABLE I. Reference QFV scenario: shown are the basic MSSM parameters at $Q = 125.5$ GeV $\simeq m_{h^0}$, except for m_{A^0} which is the pole mass (i.e. the physical mass) of A^0, with $T_{U33} = -2050$ GeV (corresponding to $\delta_{33}^{uRL} = -0.2$). All other squark parameters not shown here are zero.

M_1	M_2	M_3
250 GeV	500 GeV	1500 GeV

μ	$\tan\beta$	m_{A^0}
2000 GeV	20	1500 GeV

	$\alpha = 1$	$\alpha = 2$	$\alpha = 3$
$M^2_{Q\alpha\alpha}$	$(2400)^2$ GeV^2	$(2360)^2$ GeV^2	$(1850)^2$ GeV^2
$M^2_{U\alpha\alpha}$	$(2380)^2$ GeV^2	$(1050)^2$ GeV^2	$(950)^2$ GeV^2
$M^2_{D\alpha\alpha}$	$(2380)^2$ GeV^2	$(2340)^2$ GeV^2	$(2300)^2$ GeV^2

δ_{23}^{LL}	δ_{23}^{uRR}	δ_{23}^{uRL}	δ_{23}^{uLR}
0.05	0.2	0.03	0.06

TABLE II. Physical masses in GeV of the particles for the scenario of Table I.

$m_{\tilde{\chi}_1^0}$	$m_{\tilde{\chi}_2^0}$	$m_{\tilde{\chi}_3^0}$	$m_{\tilde{\chi}_4^0}$	$m_{\tilde{\chi}_1^+}$	$m_{\tilde{\chi}_2^+}$
260	534	2020	2021	534	2022

m_{h^0}	m_{H^0}	m_{A^0}	m_{H^+}
126.08	1498	1500	1501

$m_{\tilde{g}}$	$m_{\tilde{u}_1}$	$m_{\tilde{u}_2}$	$m_{\tilde{u}_3}$	$m_{\tilde{u}_4}$	$m_{\tilde{u}_5}$	$m_{\tilde{u}_6}$
1473	756	965	1800	2298	2301	2332

TABLE III. Flavor decomposition of $\tilde{u}_1$ and $\tilde{u}_2$ for the scenario of Table I. Shown are the squared coefficients.

	$\tilde{u}_L$	$\tilde{c}_L$	$\tilde{t}_L$	$\tilde{u}_R$	$\tilde{c}_R$	$\tilde{t}_R$
$\tilde{u}_1$	0	0.0004	0.012	0	0.519	0.468
$\tilde{u}_2$	0	0.0004	0.009	0	0.480	0.509

TABLE IV. Constraints on the MSSM parameters from the B-physics experiments relevant mainly for the mixing between the second and the third generations of squarks and from the data on the h^0 mass. The fourth column shows constraints at 95% C.L. obtained by combining the experimental error quadratically with the theoretical uncertainty, except for m_{h^0}.

Observable	Experimental data	Theoretical uncertainty	Constraint (95% C.L.)
ΔM_{B_s} [ps^{-1}]	17.768 ± 0.024 (68% C.L.) [36]	± 3.3 (95% C.L.) [37,38]	17.77 ± 3.30
$10^4 \times \mathrm{B}(b \to s\gamma)$	3.40 ± 0.21 (68% C.L.) [39]	± 0.23 (68% C.L.) [40]	3.40 ± 0.61
$10^6 \times \mathrm{B}(b \to s l^+ l^-)$ ($l = e$ or μ)	$1.60^{+0.48}_{-0.45}$ (68% C.L.) [41]	± 0.11 (68% C.L.) [42]	$1.60^{+0.97}_{-0.91}$
$10^9 \times \mathrm{B}(B_s \to \mu^+\mu^-)$	2.9 ± 0.7 (68% C.L.) [43–45]	± 0.23 (68% C.L.) [46]	2.90 ± 1.44
$10^4 \times \mathrm{B}(B^+ \to \tau^+\nu)$	1.15 ± 0.23 (68% C.L.) [47–49]	± 0.29 (68% C.L.) [47]	1.15 ± 0.73
m_{h^0} [GeV]	125.03 ± 0.30 (68% C.L.) (CMS) [3], 125.36 ± 0.41 (68% C.L.) (ATLAS) [1]	± 2 [50]	125.15 ± 2.48

Thus, our total result can be written in the form

$$\Gamma(h^0 \to c\bar{c}) \equiv \Gamma^{\mathrm{impr}}(h^0 \to c\bar{c}) = \Gamma^{\mathrm{tree}}(m_c) + \delta\tilde{\Gamma}^g + \delta\Gamma^{\tilde{g}} + \delta\Gamma^{\mathrm{EW}}, \quad (58)$$

where the new gluon contribution $\delta\tilde{\Gamma}^g$ is given by

$$\delta\tilde{\Gamma}^g = \delta\Gamma^g(m_c|_{\mathrm{SM}}) - \Gamma^{\mathrm{tree}}(m_c)\frac{m_c^2 - m_c^2|_{\mathrm{SM}}}{m_c^2}. \quad (59)$$

IV. NUMERICAL RESULTS

To demonstrate clearly the effect of QFV in the MSSM, we have explicitly chosen a reference scenario with a rather

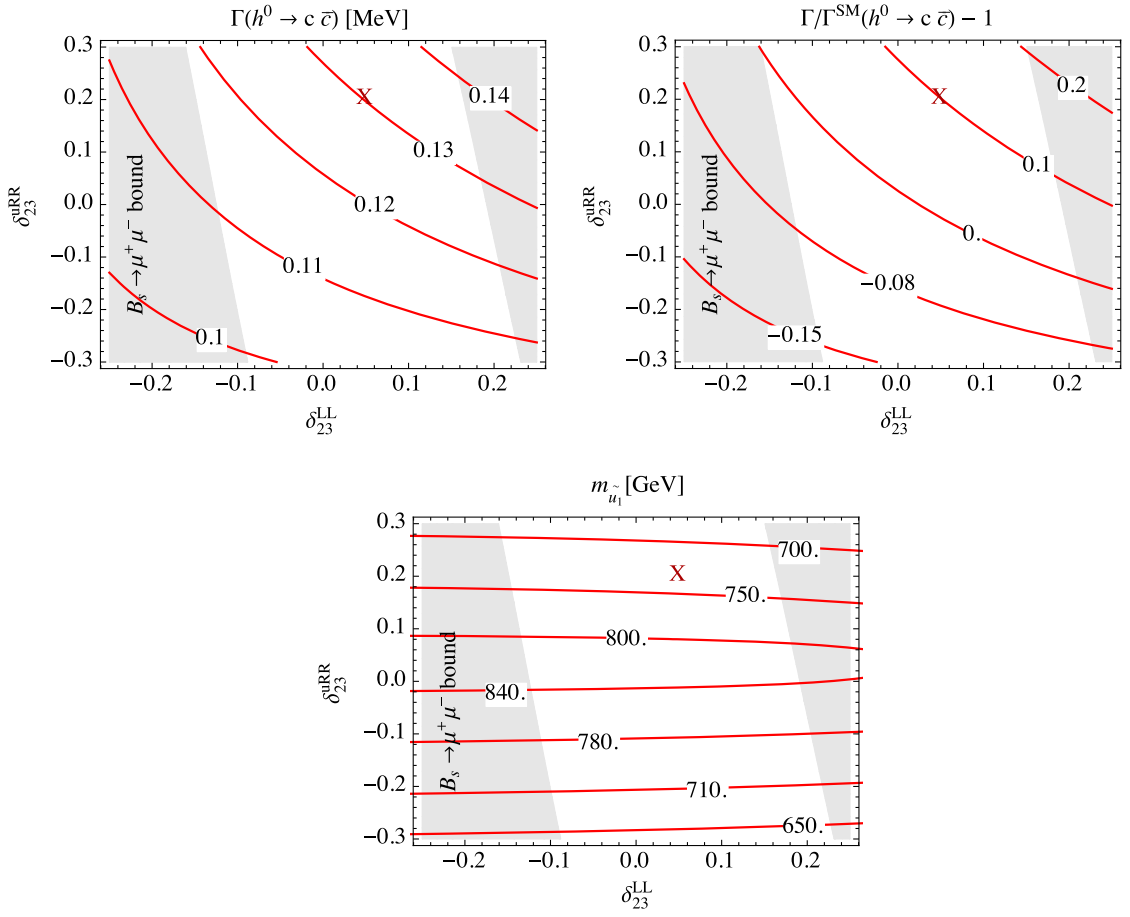

FIG. 5 (color online). Dependence on the QFV parameters δ^{LL}_{23} and δ^{uRR}_{23} of the width (a) $\Gamma(h^0 \to c\bar{c})$ in MeV, (b) $\Gamma(h^0 \to c\bar{c})/\Gamma^{\mathrm{SM}}(h^0 \to c\bar{c})$, and (c) the mass of the lightest squark $\tilde{u}_1$ in GeV. The gray region is excluded by the constraint from the $\mathrm{B}(B_s \to \mu^+\mu^-)$ data.

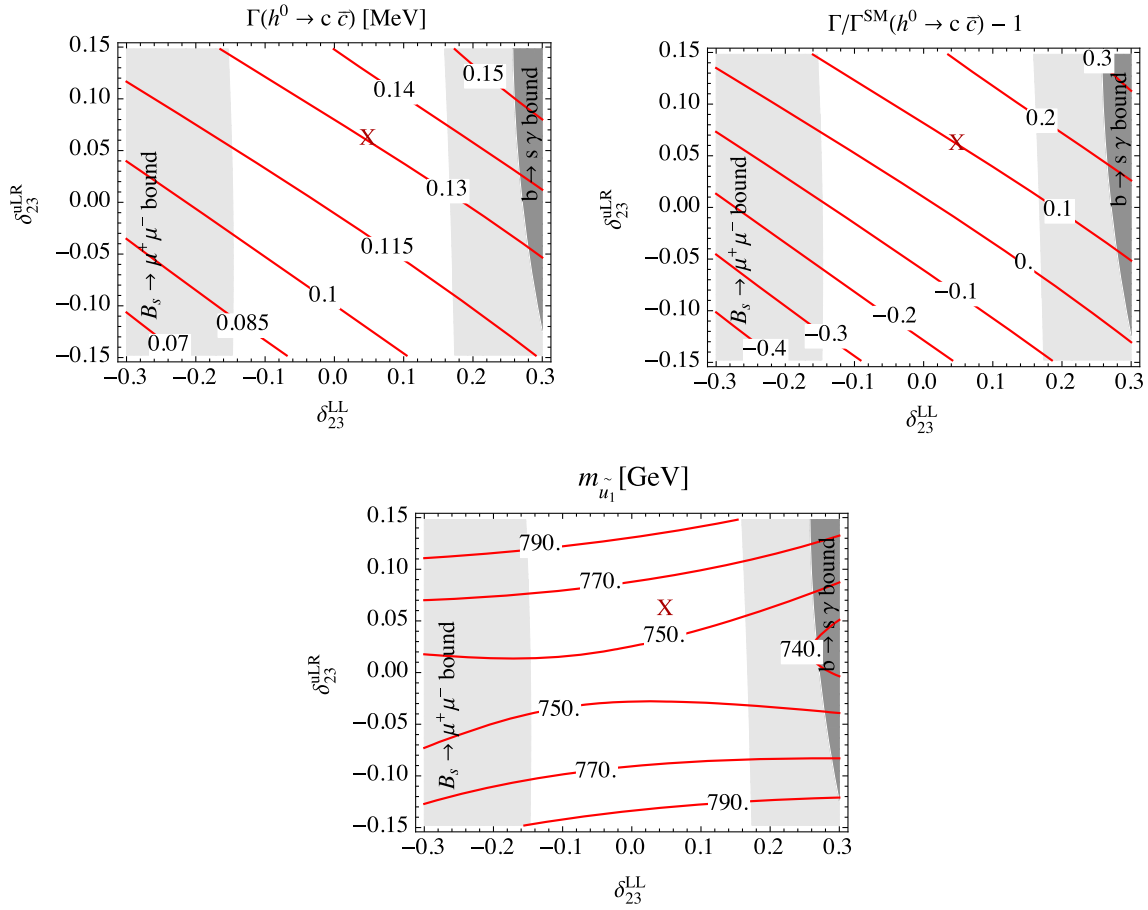

FIG. 6 (color online). Dependence on the QFV parameters δ_{23}^{LL} and δ_{23}^{uLR} of the width (a) $\Gamma(h^0 \to c\bar{c})$ in MeV, (b) $\Gamma(h^0 \to c\bar{c})/\Gamma^{\rm SM}(h^0 \to c\bar{c})$, and (c) the mass of the lightest squark $\tilde{u}_1$ in GeV. The light and dark gray regions are excluded by the constraints from the $\mathrm{B}(B_s \to \mu^+\mu^-)$ and $\mathrm{B}(b \to s\gamma)$ data, respectively.

strong $\tilde{c} - \tilde{t}$ mixing. The MSSM parameters at $Q = 125.5$ GeV $\simeq m_{h^0}$ are given in Table I.

The resulting physical masses of the particles are shown in Table II. The flavor decomposition of the two lighter squarks $\tilde{u}_1$ and $\tilde{u}_2$ can be seen in Table III. This scenario satisfies all present experimental and theoretical constraints given in Appendix D. For calculating the masses and the mixing, as well as the low-energy observables, especially those in the B meson sector (see Table IV), we use the public code SPheno v3.3.3 [30,31]. The width $\Gamma(h^0 \to c\bar{c})$ at full one-loop level in the MSSM with QFV is calculated on the basis of the formulas given above with the help of FeynArts [33] and FormCalc [34]. We also use the SSP package [35]. In the following plots, we show the QFV parameter dependences of the full one-loop level width $\Gamma(h^0 \to c\bar{c})$ of Eq. (58) around the reference point of Table I.

In Figs. 5(a) and 5(b), we show the dependence of the width $\Gamma(h^0 \to c\bar{c})$ on the QFV parameters δ_{23}^{LL} ($\tilde{c}_L - \tilde{t}_L$ mixing) and δ_{23}^{uRR} ($\tilde{c}_R - \tilde{t}_R$ mixing), with the other parameters fixed as in Table I. In Fig. 5(a) we show the width in MeV as a function of δ_{23}^{LL} and δ_{23}^{uRR}. The white area is the region allowed by all the constraints of Appendix D, with the reference point of Table I indicated by X. In the allowed region, this width can vary from 0.1 to 0.14 MeV. As can be seen, there is a rather strong dependence on δ_{23}^{uRR}.

In Fig. 5(b) we show the deviation of the $\Gamma(h^0 \to c\bar{c})$ from the SM width $\Gamma^{\rm SM}(h^0 \to c\bar{c}) = 0.118$ MeV [8]. This deviation varies between -15% and 20%. It is interesting to mention that we obtain $\Gamma^{\rm QFC}(h^0 \to c\bar{c}) = 0.116$ MeV for the full one-loop width in the QFC MSSM case for our reference scenario corresponding to Table I. This means that the QFC supersymmetric contributions change the width $\Gamma(h^0 \to c\bar{c})$ by only $\sim -15\%$ compared to the SM value. Comparing our QFC one-loop result with FeynHiggs-2.10.2 [51], we have a difference less than 1%. Note that the mass of the lightest squark $\tilde{u}_1$ can vary in the allowed region between 650 and 850 GeV, as seen in Fig. 5(c). Note also that in Figs. 5(a) and 5(b) the QFV parameter $-0.3 < \delta_{23}^{uRR} < 0.3$ is not restricted by the constraints from the B sector but from the mass of the lightest stop [corresponding to the lightest squark mass shown in Fig. 5(c)] and the lightest neutralino (see Table II) in the context of the simplified MSSM with QFC [52]. In principle, this

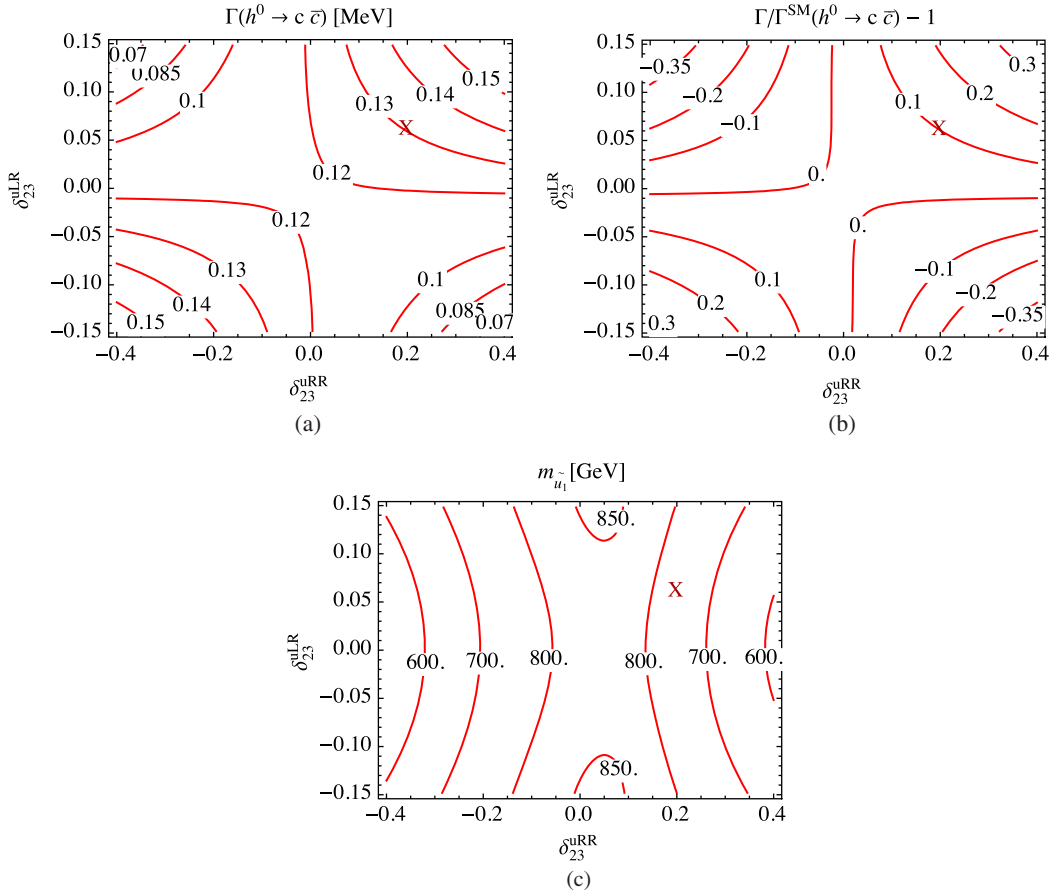

FIG. 7 (color online). Dependence on the QFV parameters δ_{23}^{uRR} and δ_{23}^{uLR} of the width (a) $\Gamma(h^0 \to c\bar{c})$ in MeV, (b) $\Gamma(h^0 \to c\bar{c})/\Gamma^{\mathrm{SM}}(h^0 \to c\bar{c})$, and (c) the mass of the lightest squark $\tilde{u}_1$ in GeV.

experimental restriction on the lightest stop mass does not hold for the case of QFV, and a wider range of δ_{23}^{uRR} is allowed [53].

In Figs. 6(a) and 6(b), we show the dependence of the width $\Gamma(h^0 \to c\bar{c})$ on the QFV parameters δ_{23}^{LL} and δ_{23}^{uLR} ($\tilde{c}_L - \tilde{t}_R$ mixing) with the other parameters fixed as in Table I. In the allowed range the width can vary between 0.08 and 0.15 MeV. The deviation of $\Gamma(h^0 \to c\bar{c})$ from the SM value $\Gamma^{\mathrm{SM}}(h^0 \to c\bar{c})$ lies between -30% and 25% [Fig. 6(b)]. Figure 6(c) shows the dependence of the mass $m_{\tilde{u}_1}$.

In analogy we show in Fig. 7 the corresponding plots for the dependences on the QFV parameters δ_{23}^{uRR} and δ_{23}^{uLR}. As seen in Fig. 7(a), the width $\Gamma(h^0 \to c\bar{c})$ varies in the allowed region between 0.07 and 0.15 MeV. The deviation from the SM value $\Gamma^{\mathrm{SM}}(h^0 \to c\bar{c})$ is between -35% and 30% [see Fig. 7(b)]. The mass of $\tilde{u}_1$ varies between 600 and 850 GeV, as seen in Fig. 7(c).

In Fig. 8 we show the dependence of $\delta\Gamma^X/\Gamma^{\mathrm{SM}}(h^0 \to c\bar{c})$ on the QFV parameters $\delta_{23}^{uRR}, \delta_{23}^{LL}, \delta_{23}^{uLR}$, and δ_{23}^{uRL} for the reference scenario of Table I, where $\delta\Gamma^X$ denotes the individual contribution of $X = (g, \mathrm{impr}), \tilde{g}, \mathrm{EW}$ (including the EW MSSM contributions) to the width $\Gamma(h^0 \to c\bar{c})$ [see Eq. (58)]. As can be seen, the gluino loop contribution $\delta\Gamma^{\tilde{g}}$ depends significantly on δ_{23}^{uRR} and δ_{23}^{uLR} with the dependences on δ_{23}^{LL} and δ_{23}^{uRL} being somewhat weaker. The gluino loop contribution $\delta\Gamma^{\tilde{g}}/\Gamma^{\mathrm{SM}}$ can go up to 45% [see Figs. 8(a) and 8(d)]. It can also be seen that the electroweak loop contributions $\delta\Gamma^{\mathrm{EW}}$ cannot be neglected with $\delta\Gamma^{\mathrm{EW}}/\Gamma^{\mathrm{SM}}$ being around 5%. Clearly, its dependence on the QFV parameters is weak.

The strong dependences of the width $\Gamma(h^0 \to c\bar{c})$ on the QFV parameters shown in this section can be explained as follows. First of all, the scenario chosen is characterized by large QFV parameters, which in our case are the large $\tilde{c}_{L,R} - \tilde{t}_{L,R}$ mixing parameters $\delta_{23}^{LL}, \delta_{23}^{uRR}, \delta_{23}^{uRL}, \delta_{23}^{uLR}$, and particularly large QFV trilinear couplings T_{U23}, T_{U32} (note that $\delta_{23}^{uRL} \sim T_{U23}$ and $\delta_{23}^{uLR} \sim T_{U32}$). In such a scenario, the lightest up-type squarks $\tilde{u}_{1,2}$ are strong admixtures of $\tilde{c}_{L,R} - \tilde{t}_{L,R}$, and, hence, the couplings $\tilde{u}_{1,2}\tilde{u}_{1,2}^* h^0$ ($\sim \mathrm{Re}(H_2^0)$) in Fig. 3 are strongly enhanced; see Eq. (A3). In addition, large $\tilde{t}_L - \tilde{t}_R$ mixing due to the large QFC trilinear coupling T_{U33} occurs. Moreover, the $\tilde{t}_L\tilde{t}_L^* h^0$ and $\tilde{t}_R\tilde{t}_R^* h^0$ couplings are proportional to the top-quark mass squared [see Eq. (A3)], which additionally enhances the $\tilde{u}_{1,2}\tilde{u}_{1,2}^* h^0$ couplings and thus also the vertex gluino contributions of Fig. 3 in case of QFV.

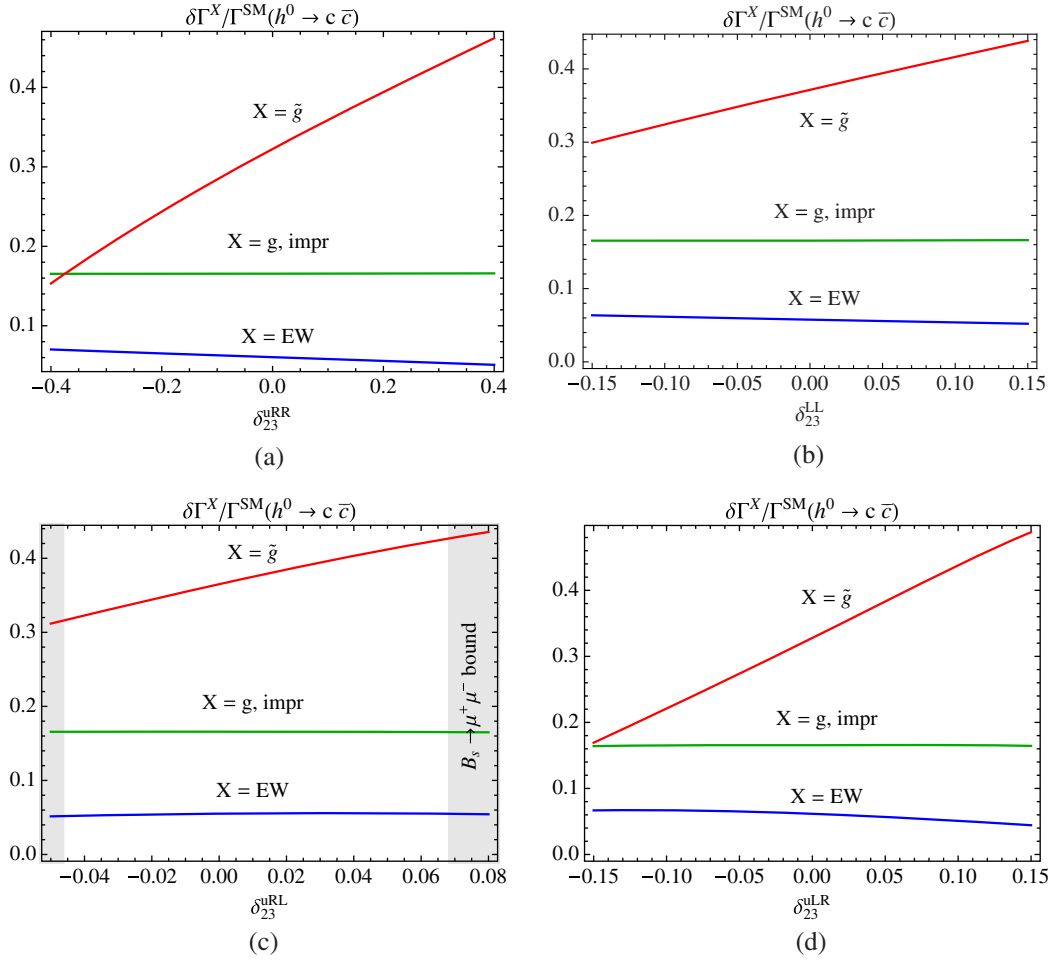

FIG. 8 (color online). Dependences on the QFV parameters of the one-loop $\tilde{g}$, EW, and improved g contributions to the width $\Gamma(h^0 \to c\bar{c})$. Note that for the $\tilde{g}$ and EW contributions only the one-loop scale independent part is shown as in the $\overline{\text{DR}}$ scheme the scale dependent part cancels with the tree-level scale dependent part.

V. OBSERVABILITY OF THE DEVIATION OF $\Gamma(h^0 \to c\bar{c})$ FROM ITS SM VALUE AT THE ILC

Observation of any significant deviation of the width $\Gamma(h^0 \to c\bar{c})$ from its SM prediction signals new physics beyond the SM. It is important to estimate the uncertainties of the SM prediction reliably in order to confirm such a deviation. Once the deviation is discovered, one has to work out the new physics candidates suggesting it.

The uncertainties of the SM prediction come from two sources [54–57]. One is the parametric uncertainty, and the other is the theory uncertainty. The former is due to the errors of the SM input parameters such as $m_c(m_c)|_{\overline{\text{MS}}}$ and $\alpha_s(m_Z)|_{\overline{\text{MS}}}$, and the latter is due to unknown higher-order corrections. The theory uncertainty is estimated mainly by renormalization-scale dependence uncertainties which are indicative of not knowing higher-order terms in a perturbative expansion of the corresponding observable. These scale dependence uncertainties are estimated by varying the scale Q from Q/2 to 2Q [54–56]. (Note that in our case $\text{Q} = m_{h^0}$.)

To estimate the uncertainty of the width $\Gamma(h^0 \to c\bar{c})$ in the MSSM with QFV at our reference point, we proceed in an analogous way. We calculate the parametric uncertainty in the width $\Gamma(h^0 \to c\bar{c})$ due to errors in the inputs $m_c(m_c)|_{\overline{\text{MS}}}$ and $\alpha_s(m_Z)|_{\overline{\text{MS}}}$ following [58]

$$\frac{\delta\Gamma}{\Gamma} = \left|\frac{m_c}{\Gamma}\frac{\partial\Gamma}{\partial m_c}\right|\frac{\delta m_c}{m_c} \oplus \left|\frac{\alpha_s}{\Gamma}\frac{\partial\Gamma}{\partial\alpha_s}\right|\frac{\delta\alpha_s}{\alpha_s}, \tag{60}$$

where as input we take $m_c(m_c)|_{\overline{\text{MS}}} = 1.275$ GeV with $\delta m_c/m_c = 2\%$ [39], and $\alpha_s(m_Z)|_{\overline{\text{MS}}} = 0.1185$ with $\delta\alpha_s/\alpha_s = 0.5\%$ [59]. $\delta\text{X}/\text{X}$ denotes the relative error of the quantity X. At our reference point of Table I, we get

$$\frac{\delta\Gamma}{\Gamma} = |2.6|\frac{\delta m_c}{m_c} \oplus |-4.0|\frac{\delta\alpha_s}{\alpha_s} = 5.2\% \oplus 2\%. \tag{61}$$

Note that the parametric uncertainties due to errors of the other SM input parameters, such as m_b, are negligible.

The theory uncertainty of the width for our reference point is shown on Fig. 9. We have $\delta\Gamma/\Gamma(h^0 \to c\bar{c}) = {}^{-0.46\%}_{+0.11\%}$, where $\Gamma(h^0 \to c\bar{c})$ is the improved one-loop corrected

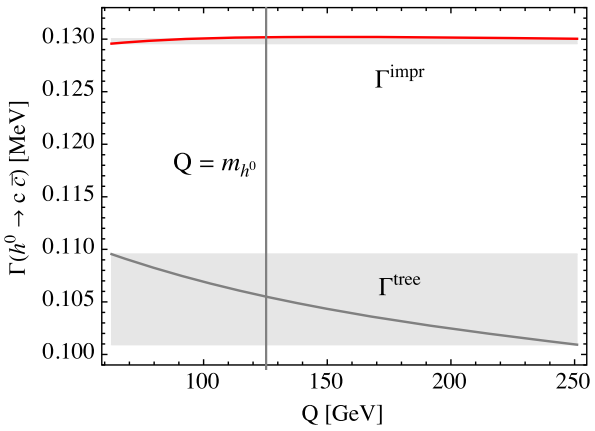

FIG. 9 (color online). Renormalization-scale dependence of $\Gamma(h^0 \to c\bar{c})$. $\Gamma^{\rm impr}(h^0 \to c\bar{c})$ is the improved one-loop corrected width of Eq. (58). The vertical line shows $Q = m_{h^0}$.

width of Eq. (58). Thus, for this uncertainty, we take ∼0.5%.

For the total error in the width at our reference point, we get

$$\sqrt{5.2\%^2 + 2\%^2} + 0.5\% \approx 6.1\%, \tag{62}$$

where the parametric uncertainties are added quadratically and the theory uncertainty is added to them linearly. The obtained total uncertainty (62) at our reference point is $\sim \pm 6.1\%$ (at 68% C.L.), which is in good agreement with the estimated total uncertainty of $\Gamma^{\rm SM}(h^0 \to c\bar{c})$; see Table 13 of Ref. [56]. Note that the uncertainty in the coupling is half of the uncertainty in the width.

As seen in Sec. IV, the deviation $\Gamma(h^0 \to c\bar{c})/\Gamma^{\rm SM}(h^0 \to c\bar{c})$ can be as large as $\sim \pm 35\%$. Such a large deviation can be observed at the ILC (500 GeV) with 1600 (500) fb^{-1}, where the expected experimental error in the width is ∼3% (5.6%) [60,61]. A measurement of $\Gamma(h^0 \to c\bar{c})$ at LHC (even with the high luminosity upgrade) is demanding due to uncertainties in the charm tagging.

VI. CONCLUSIONS

We have calculated the width $\Gamma(h^0 \to c\bar{c})$ at full one-loop level within the MSSM with quark flavor violation. In particular, we have studied $\tilde{c}_{R,L} - \tilde{t}_{R,L}$ mixing, taking into account the experimental constraints from B-physics, m_{h^0}, and SUSY particle searches. The width $\Gamma(h \to c\bar{c})$ turns out to be very sensitive to $\tilde{c}_{R,L} - \tilde{t}_{R,L}$ mixing.

In our calculation we have used the $\overline{\rm DR}$ renormalization scheme. In particular, we have derived the explicit formula for the dominant gluino loop contribution. We also have performed a detailed numerical study of the QFV parameter dependence of the width. Whereas the width $\Gamma(h^0 \to c\bar{c})$ in the QFC MSSM case is only slightly different from its SM value, in the QFV case, this width can deviate from the SM by up to $\sim \pm 35\%$.

We have estimated the theoretical uncertainties of $\Gamma(h^0 \to c\bar{c})$ and have shown that the SUSY QFV contribution to this width can be observed at the ILC.

ACKNOWLEDGMENTS

We would like to thank W. Porod for helpful discussions, especially for the permanent support concerning SPheno. K. H. thanks Prof. Koji Hashimoto for the warm hospitality at RIKEN Nishina Center for Accelerator-Based Science. This work is supported by the "Fonds zur Förderung der wissenschaftlichen Forschung (FWF)" of Austria, Project No. P26338-N27.

APPENDIX A: INTERACTION LAGRANGIAN

(i) The interaction of the lightest neutral Higgs boson, h^0, with two charm quarks is given by

$$\mathcal{L}_{h^0 c\bar{c}} = s_1^c h^0 c\bar{c}, \tag{A1}$$

where the tree-level coupling s_1^c is given by Eq. (10).

(ii) In the super-CKM basis, the interaction of the lightest neutral Higgs boson, h^0, with two up-type squarks is given by

$$\mathcal{L}_{h^0 \tilde{u}_i \tilde{u}_j} = G^{\tilde{u}}_{ij1} h^0 \tilde{u}_i^* \tilde{u}_j, \quad i,j = 1,\ldots,6. \tag{A2}$$

The coupling $G^{\tilde{u}}_{ij1}$ reads

$$\begin{aligned} G^{\tilde{u}}_{ij1} = -\frac{g}{2m_W}\Bigg[& -m_W^2 \sin(\alpha+\beta)\left[\left(1 - \frac{1}{3}\tan^2\theta_W\right)(U^{\tilde{u}})_{jk}(U^{\tilde{u}*})_{ik} + \frac{4}{3}\tan^2\theta_W (U^{\tilde{u}})_{j(k+3)}(U^{\tilde{u}*})_{i(k+3)}\right] \\ & + 2\frac{\cos\alpha}{\sin\beta}\left[(U^{\tilde{u}})_{jk} m^2_{u,k}(U^{\tilde{u}*})_{ik} + (U^{\tilde{u}})_{j(k+3)} m^2_{u,k}(U^{\tilde{u}*})_{i(k+3)}\right] \\ & + \frac{\sin\alpha}{\sin\beta}\left[\mu^*(U^{\tilde{u}})_{j(k+3)} m_{u,k}(U^{\tilde{u}*})_{ik} + \mu(U^{\tilde{u}})_{jk} m_{u,k}(U^{\tilde{u}*})_{i(k+3)}\right] \\ & + \frac{\cos\alpha}{\sin\beta}\frac{v_2}{\sqrt{2}}\left[(U^{\tilde{u}})_{j(k+3)}(T_U)_{kl}(U^{\tilde{u}*})_{il} + (U^{\tilde{u}})_{jk}(T_U^*)_{lk}(U^{\tilde{u}*})_{i(l+3)}\right]\Bigg], \end{aligned} \tag{A3}$$

where the sum over $k, l = 1, 2, 3$ is understood. Here $U^{\tilde{u}}$ is the mixing matrix of the up-type squarks

$$\tilde{u}_{iL} = (U^{\tilde{u}\dagger})_{ik}\tilde{u}_k, \qquad \tilde{u}_{iR} = (U^{\tilde{u}\dagger})_{(i+3)k}\tilde{u}_k, \quad i = 1, 2, 3, \quad k = 1, \ldots, 6. \tag{A4}$$

Note that $(T_U)_{kl}$ in (A3) are given in the SUSY Les Houche Accord notation[62].

(iii) The interaction of gluino, up-type squark, and a charm quark is described by

$$\mathcal{L}_{\tilde{g}\tilde{u}_i c} = -\sqrt{2}g_s T^{\alpha}_{rs}\left[\bar{\tilde{g}}^{\alpha}\left(U^{\tilde{u}}_{i2}e^{-i\frac{\phi_3}{2}}P_L - U^{\tilde{u}}_{i5}e^{i\frac{\phi_3}{2}}P_R\right)c^s\tilde{u}_i^{*,r} + \bar{c}^r\left(U^{\tilde{u}*}_{i2}e^{i\frac{\phi_3}{2}}P_R - U^{\tilde{u}*}_{i5}e^{-i\frac{\phi_3}{2}}P_L\right)\tilde{g}^{\alpha}\tilde{u}_i^s\right], \tag{A5}$$

where T^{α} are the SU(3) colour group generators and summation over $r, s = 1, 2, 3$ and over $\alpha = 1, \ldots, 8$ is understood. In our case the parameter $M_3 = m_{\tilde{g}}e^{i\phi_3}$ is taken as real, $\phi_3 = 0$.

APPENDIX B: HARD GLUON/PHOTON BREMSSTRAHLUNG

The convergent one-loop gluon/photon corrected decay width in the limit of vanishing gluon/photon mass, $\lambda = 0$, is given by

$$\Gamma^{g/\gamma}(h^0 \to c\bar{c}) = \Gamma^{\text{tree}} + \delta\Gamma^{g/\gamma} + \Gamma^{\text{hard}}(h^0 \to c\bar{c}g/\gamma). \tag{B1}$$

The hard gluon radiation width reads

$$\Gamma^{\text{hard}}(h^0 \to c\bar{c}g) = \frac{2\alpha_s|s_1^c|^2}{\pi^2 m_{h^0}}[J_1 - (m_{h^0}^2 - 4m_c^2) \times (J_2 - (m_{h^0}^2 - 2m_c^2)J_3)], \tag{B2}$$

with the integrals [63]

$$J_1 = \frac{1}{8m_{h^0}^2}\left((\kappa^2 + 6m_c^4)\ln\beta_0 - \frac{3}{2}\kappa(m_{h^0}^2 - 2m_c^2)\right), \tag{B3}$$

$$J_2 = \frac{1}{4m_{h^0}^2}\left(2\kappa\ln\left(\frac{\kappa^2}{\lambda m_{h^0}m_c^2}\right) - 4\kappa - m_{h^0}^2\ln\beta_0\right), \tag{B4}$$

$$J_3 = \frac{1}{2m_{h^0}^2}\left(-\ln\left(\frac{\lambda m_{h^0}m_c^2}{\kappa^2}\right)\ln\beta_0 + \ln^2\beta_0 - \ln^2\beta_1 + \text{Li}_2(1-\beta_0^2) - \text{Li}_2(1-\beta_1^2)\right), \tag{B5}$$

where $\text{Li}_s(z)$ is the polylogarithm function, defined by the infinite sum

$$\text{Li}_s(z) = \sum_{k=1}^{\infty}\frac{z^k}{k^s}, \tag{B6}$$

$$\beta_0 = \frac{m_{h^0}^2 - 2m_c^2 + \kappa}{2m_c^2}, \qquad \beta_1 = \frac{m_{h^0}^2 - \kappa}{2m_{h^0}m_c}, \tag{B7}$$

$$\kappa \equiv \kappa(m_{h^0}^2, m_c^2, m_c^2) = m_{h^0}\sqrt{1 - \frac{4m_c^2}{m_{h^0}^2}}. \tag{B8}$$

The expression for the hard photon radiation width $\Gamma^{\text{hard}}(h^0 \to c\bar{c}\gamma)$ is obtained from (B2) by making the replacements $C_F = 4/3 \to e_c^2 = 4/9$ and $\alpha_s \to \alpha = e^2/(4\pi)$.

APPENDIX C: SIMPLIFIED FORMULAS FOR THE TWO- AND THREE-POINT FUNCTIONS

In our analytic calculations, we neglect the squared masses of the charm quark and the lightest neutral Higgs boson, m_c^2 and $m_{h^0}^2$, in comparison to the squared masses of the scalar quarks and the gluino, $m_{\tilde{q}_i}^2$ and $m_{\tilde{g}}^2$. In the following we list the simplified expressions for the two- and three-point functions for this case:

$$B_0(0, m_1^2, m_2^2) = \Delta + 1 + \frac{m_2^2\ln\frac{m_2^2}{Q^2} - m_1^2\ln\frac{m_1^2}{Q^2}}{m_1^2 - m_2^2} \tag{C1}$$

$$\begin{aligned} B_1(0, m_1^2, m_2^2) &= -\frac{\Delta}{2} + \frac{1}{2}\left(\ln\frac{m_2^2}{Q^2} - \frac{m_1^4}{(m_1^2 - m_2^2)^2}\ln\frac{m_2^2}{m_1^2} + \frac{m_2^2 - 3m_1^2}{2(m_1^2 - m_2^2)}\right) \\ &= -\frac{\Delta}{2} + \frac{1}{4}\left(\ln\frac{m_1^2}{Q^2} + \ln\frac{m_2^2}{Q^2} - \frac{m_1^4 + 2m_1^2m_2^2 - m_2^4}{(m_1^2 - m_2^2)^2} \times \ln\frac{m_2^2}{m_1^2} + \frac{m_2^2 - 3m_1^2}{m_1^2 - m_2^2}\right) \end{aligned} \tag{C2}$$

$$B_0(0, m^2, 0) = \Delta + 1 - \ln\frac{m^2}{Q^2} \tag{C3}$$

$$B_1(0, m^2, 0) = \frac{-\Delta + \ln\frac{m^2}{Q^2}}{2} - \frac{3}{4} \tag{C4}$$

$$B_0(0, m^2, m^2) = B_0(0, m^2, 0) - 1 = \Delta - \ln\frac{m^2}{Q^2} \tag{C5}$$

$$B_1(0, m^2, m^2) = -\frac{1}{2}B_0(0, m^2, m^2) \tag{C6}$$

$$B_0(m^2, 0, m^2) = \Delta + 2 + \ln\frac{Q^2}{m^2} \tag{C7}$$

$$B_1(m^2, 0, m^2) = -\frac{1}{2}\left(\Delta + 1 + \ln\frac{Q^2}{m^2}\right), \tag{C8}$$

with Δ the UV divergence factor and Q the renormalization scale,

$$\dot{B}_0(0, m_1^2, m_2^2) = \frac{m_1^4 - m_2^4 + 2m_2^2 m_1^2 \ln\frac{m_2^2}{m_1^2}}{2(m_1^2 - m_2^2)^3} \tag{C9}$$

$$\dot{B}_1(0, m_1^2, m_2^2) = -\frac{2m_1^6 + 3m_2^2 m_1^4 - 6m_2^4 m_1^2 + m_2^6 + 6m_2^2 m_1^4 \ln\frac{m_2^2}{m_1^2}}{6(m_1^2 - m_2^2)^4} \tag{C10}$$

$$\dot{B}_0(0, m^2, m^2) = \frac{1}{6m^2} \tag{C11}$$

$$\dot{B}_0(0, m^2, 0) = \frac{1}{2m^2} \tag{C12}$$

$$\dot{B}_0(m^2, \lambda^2, m^2) = -\frac{1}{2m^2}\left(2 - \ln\frac{m^2}{\lambda^2}\right) \tag{C13}$$

$$\dot{B}_1(m^2, \lambda^2, m^2) = -\frac{1}{2m^2} \tag{C14}$$

$$C_0(m_1^2, m_2^2, , m_1^2, \lambda^2, m_1^2, m_1^2) = \frac{1}{m_2^2\beta}\left[\ln\frac{1+\beta}{1-\beta}\ln\frac{m_2^2\beta}{\lambda^2} - \frac{2\pi^2}{3} - 2\mathrm{Li}_2\left(\frac{1+\beta}{1-\beta}\right)^{1/2} - 2\ln^2\left(\frac{1+\beta}{1-\beta}\right)^{1/2} + \ln\beta\ln\frac{1+\beta}{1-\beta}\right] \tag{C15}$$

$$C_1(m_1^2, m_2^2, , m_1^2, \lambda^2, m_1^2, m_1^2) = \frac{1}{m_2^2\beta}\ln\frac{1+\beta}{1-\beta}, \tag{C16}$$

where $\beta = (1 - 4m_1^2/m_2^2)^{1/2}$ and $\mathrm{Li}_s(z)$ is defined with (B6),

$$C_0(0,0,0,m_1^2,m_2^2,m_3^2) = \frac{B_0(0,m_1^2,m_3^2) - B_0(0,m_2^2,m_3^2)}{m_1^2 - m_2^2} = \frac{m_1^2 m_2^2 \ln\frac{m_1^2}{m_2^2} + m_2^2 m_3^2 \ln\frac{m_2^2}{m_3^2} + m_3^2 m_1^2 \ln\frac{m_3^2}{m_1^2}}{(m_1^2 - m_2^2)(m_2^2 - m_3^2)(m_1^2 - m_3^2)} \tag{C17}$$

$$C_0(0,0,0,m_1^2,m_2^2,m_2^2) = \frac{m_1^2 - m_2^2 + m_1^2 \ln\frac{m_2^2}{m_1^2}}{(m_1^2 - m_2^2)^2}. \tag{C18}$$

For $m_3 = m_2 \ll m_1$ we get

$$C_0(0,0,0,m_1^2,m_2^2,m_2^2) = \frac{1 + \ln\frac{m_2^2}{m_1^2}}{m_1^2} = \frac{1}{m_1^2} - \frac{\ln m_1^2}{m_1^2} + \frac{\ln m_2^2}{m_1^2} \tag{C19}$$

$$C_0(0,0,0,m^2,m^2,m^2) = -\frac{1}{2m^2}. \tag{C20}$$

Note that the expression (C19) vanishes for fixed m_2 and $m_1 \to \infty$.

APPENDIX D: THEORETICAL AND EXPERIMENTAL CONSTRAINTS

Here we summarize the experimental and theoretical constraints taken into account in the present paper. The constraints on the MSSM parameters from the B-physics experiments and from the Higgs boson measurement at LHC are shown in Table IV.

The *BABAR* and Belle collaborations have reported a slight excess of $\mathrm{B}(B \to D\tau\nu)$ and $\mathrm{B}(B \to D^*\tau\nu)$ [64–66]. However, it has been argued in Ref. [67] that within the MSSM this cannot be explained without being at the same time in conflict with $\mathrm{B}(B_u \to \tau\nu)$. Using the program SUSY_FLAVOR [68] we have checked that in our MSSM scenarios no significant enhancement occurs for $\mathrm{B}(B \to D\tau\nu)$. However, as pointed out in Ref. [69], the theoretical predictions (in the SM and MSSM) on $\mathrm{B}(B \to Dl\nu)$ and $\mathrm{B}(B \to D^* l\nu)$ $(l = \tau, \mu, e)$ have potentially large theoretical uncertainties due to the theoretical assumptions on the form factors at the BDW^+ and BD^*W^+ vertices (also at the BDH^+ and BD^*H^+ vertices in the MSSM). Hence the constraints from these decays are unclear. Therefore, we do not take these constraints into account in our paper.

In Ref. [70] the QFV decays $t \to qh$ with $q = u, c$, have been studied in the general MSSM with QFV. It is found that these decays cannot be visible at the current LHC runs due to the very small decay branching ratios $B(t \to qh)$.

For the mass of the Higgs boson h^0, taking the naive combination of the ATLAS and CMS measurements [1,3] $m_{h^0} = 125.15 \pm 0.24$ GeV [5] and adding the theoretical uncertainty of $\sim \pm 2$ GeV [50] linearly to the experimental uncertainty at 2σ, we take $m_{h^0} = 125.15 \pm 2.48$ GeV.

In addition to these constraints, we also require our scenarios to be consistent with the following experimental constraints:

(i) The LHC limits on the squark and gluino masses (at 95% C.L.) [52,71–92]: In the context of simplified models, gluino masses $m_{\tilde{g}} \lesssim 1$ TeV are excluded at 95% C.L. The mass limit varies in the range 1000–1400 GeV depending on assumptions. First- and second-generation squark masses are excluded below 900 GeV. Bottom squarks are excluded below 600 GeV. A typical top-squark mass limit is ~700 GeV. In Refs. [91,92] a limit for the mass

of the top-squark $m_{\tilde{t}} \gtrsim 500$ GeV for $m_{\tilde{t}} - m_{\rm LSP} = 200$ GeV is quoted. Including mixing of $\tilde{c}_R$ and $\tilde{t}_R$ would even lower this limit [53].

(ii) The LHC limits on $m_{\tilde{\chi}_1^\pm}$ and $m_{\tilde{\chi}_1^0}$ from negative searches for charginos and neutralinos mainly in leptonic final states [52,93,94].

(iii) The constraint on $(m_{A^0,H^+}, \tan\beta)$ from the MSSM Higgs boson searches at LHC [1–4,95].

(iv) The experimental limit on SUSY contributions on the electroweak ρ parameter [96]: $\Delta\rho(\mathrm{SUSY}) < 0.0012$.

Furthermore, we impose the following theoretical constraints from the vacuum stability conditions for the trilinear coupling matrices [97]:

$$|T_{U\alpha\alpha}|^2 < 3Y_{U\alpha}^2(M_{Q\alpha\alpha}^2 + M_{U\alpha\alpha}^2 + m_2^2), \tag{D1}$$

$$|T_{D\alpha\alpha}|^2 < 3Y_{D\alpha}^2(M_{Q\alpha\alpha}^2 + M_{D\alpha\alpha}^2 + m_1^2), \tag{D2}$$

$$|T_{U\alpha\beta}|^2 < Y_{U\gamma}^2(M_{Q\beta\beta}^2 + M_{U\alpha\alpha}^2 + m_2^2), \tag{D3}$$

$$|T_{D\alpha\beta}|^2 < Y_{D\gamma}^2(M_{Q\beta\beta}^2 + M_{D\alpha\alpha}^2 + m_1^2), \tag{D4}$$

where $\alpha,\beta = 1,2,3$, $\alpha \neq \beta$; $\gamma = \mathrm{Max}(\alpha,\beta)$ and $m_1^2 = (m_{H^+}^2 + m_Z^2 \sin^2\theta_W)\sin^2\beta - \frac{1}{2}m_Z^2$, $m_2^2 = (m_{H^+}^2 + m_Z^2\sin^2\theta_W)\cos^2\beta - \frac{1}{2}m_Z^2$. The Yukawa couplings of the up-type and down-type quarks are $Y_{U\alpha} = \sqrt{2}m_{u_\alpha}/v_2 = \frac{g}{\sqrt{2}}\frac{m_{u_\alpha}}{m_W \sin\beta}$ $(u_\alpha = u, c, t)$ and $Y_{D\alpha} = \sqrt{2}m_{d_\alpha}/v_1 = \frac{g}{\sqrt{2}}\frac{m_{d_\alpha}}{m_W \cos\beta}$ $(d_\alpha = d, s, b)$, with m_{u_α} and m_{d_α} being the running quark masses at the weak scale and g being the SU(2) gauge coupling. All soft SUSY-breaking parameters are given at Q = 125.5 GeV. As SM parameters we take $m_Z = 91.2$ GeV and the on-shell top-quark mass $m_t = 173.3$ GeV [98]. We have found that our results shown are fairly insensitive to the precise value of m_t.

[1] G. Aad *et al.* (ATLAS Collaboration), Phys. Rev. D **90**, 052004 (2014).
[2] M. Kado, *37th International Conference on High Energy Physics, Valencia, Spain*, 2014.
[3] S. Chatrchyan *et al.* (CMS Collaboration), CMS-PAS-HIG-14-009.
[4] A. David, *37th International Conference on High Energy Physics, Valencia, Spain*, 2014.
[5] J. Ellis, *Second Annual Conference on Large Hadron Collider Physics (LHCP2014), Columbia University, New York*, 2014.
[6] S. Heinemeyer *et al.* (LHC Higgs Cross Section Working Group Collaboration), arXiv:1307.1347.
[7] A. Djouadi, Phys. Rep. **457**, 1 (2008).
[8] K. A. Olive *et al.* (Particle Data Group), Chin. Phys. C **38**, 090001 (2014).
[9] G. Bozzi, B. Fuks, B. Herrmann, and M. Klasen, Nucl. Phys. **B787**, 1 (2007).
[10] B. Fuks, B. Herrmann, and M. Klasen, Nucl. Phys. **B810**, 266 (2009).
[11] A. Bartl, H. Eberl, B. Herrmann, K. Hidaka, W. Majerotto, and W. Porod, Phys. Lett. B **698**, 380 (2011); **700**, 390(E) (2011).
[12] M. Bruhnke, B. Herrmann, and W. Porod, J. High Energy Phys. 09 (2010) 006.
[13] T. Hurth and W. Porod, J. High Energy Phys. 08 (2009) 087.
[14] A. Bartl, K. Hidaka, K. Hohenwarter-Sodek, T. Kernreiter, W. Majerotto, and W. Porod, Phys. Lett. B **679**, 260 (2009).
[15] A. Bartl, H. Eberl, E. Ginina, B. Herrmann, K. Hidaka, W. Majerotto, and W. Porod, Phys. Rev. D **84**, 115026 (2011).
[16] B. Fuks, B. Herrmann, and M. Klasen, Phys. Rev. D **86**, 015002 (2012).
[17] Y. Nomura, M. Papucci, and D. Stolarski, Phys. Rev. D **77**, 075006 (2008).
[18] B. C. Allanach *et al.*, Comput. Phys. Commun. **180**, 8 (2009).
[19] F. Gabbiani, E. Gabrielli, A. Masiero, and L. Silvestrini, Nucl. Phys. **B477**, 321 (1996).
[20] A. Dabelstein, Nucl. Phys. **B456**, 25 (1995).
[21] A. Crivellin, Phys. Rev. D **83**, 056001 (2011).
[22] A. Crivellin, L. Hofer, and , J. Rosiek , J. High Energy Phys. 07 (2011) 017.
[23] A. Crivellin and C. Greub, Phys. Rev. D **87**, 015013 (2013).
[24] J. F. Gunion and H. E. Haber, Nucl. Phys. **B272**, 1 (1986).
[25] W. Frisch, Ph.D. thesis, Vienna University of Technology, 2011, http://www.hephy.at/fileadmin/user_upload/Projekte/theorie_susy/diss_Frisch_W.pdf.
[26] E. Braaten and J. P. Leveille, Phys. Rev. D **22**, 715 (1980).
[27] M. Drees and K. Hikasa, Phys. Lett. B **240**, 455 (1990).
[28] M. Spira, Fortschr. Phys. **46**, 203 (1998).
[29] H. Eberl, K. Hidaka, S. Kraml, W. Majerotto, and Y. Yamada, Phys. Rev. D **62**, 055006 (2000).
[30] W. Porod, Comput. Phys. Commun. **153**, 275 (2003).
[31] W. Porod and F. Staub, Comput. Phys. Commun. **183**, 2458 (2012).
[32] J. A. Aguilar-Saavedra *et al.*, Eur. Phys. J. C **46**, 43 (2006).
[33] T. Hahn, Comput. Phys. Commun. **140**, 418 (2001).
[34] T. Hahn and M. Perez-Victoria, Comput. Phys. Commun. **118**, 153 (1999).
[35] F. Staub, T. Ohl, W. Porod, and C. Speckner, Comput. Phys. Commun. **183**, 2165 (2012).
[36] R. Aaij *et al.* (LHCb Collaboration), New J. Phys. **15**, 053021 (2013).
[37] M. S. Carena, A. Menon, R. Noriega-Papaqui, A. Szynkman, and C. E. M. Wagner, Phys. Rev. D **74**, 015009 (2006).
[38] P. Ball and R. Fleischer, Eur. Phys. J. C **48**, 413 (2006).

[39] J. Beringer *et al.* (Particle Data Group), Phys. Rev. D **86**, 010001 (2012).
[40] M. Misiak *et al.*, Phys. Rev. Lett. **98**, 022002 (2007).
[41] J. P. Lees *et al.* (*BABAR* Collaboration), Phys. Rev. Lett. **112**, 211802 (2014).
[42] T. Huber, T. Hurth, and E. Lunghi, Nucl. Phys. **B802**, 40 (2008).
[43] R. Aaij *et al.* (LHCb Collaboration), Phys. Rev. Lett. **111**, 101805 (2013).
[44] S. Chatrchyan *et al.* (CMS Collaboration), Phys. Rev. Lett. **111**, 101804 (2013).
[45] J. Albrecht, 37th International Conference on High Energy Physics, Valencia, Spain, 2014 (unpublished).
[46] C. Bobeth, M. Gorbahn, T. Hermann, M. Misiak, E. Stamou, and M. Steinhauser, Phys. Rev. Lett. **112**, 101801 (2014).
[47] J. M. Roney, 26th International Symposium on Lepton Photon Interactions at High Energies, San Francisco, 2013 (unpublished).
[48] J. P. Lees *et al.* (*BABAR* Collaboration), Phys. Rev. D **88**, 031102 (2013).
[49] K. Hara *et al.* (Belle Collaboration), Phys. Rev. Lett. **110**, 131801 (2013).
[50] S. Heinemeyer, O. Stal, and G. Weiglein, Phys. Lett. B **710**, 201 (2012).
[51] S. Heinemeyer, W. Hollik, and G. Weiglein, Comput. Phys. Commun. **124**, 76 (2000).
[52] F. Würthwein, 37th International Conference on High Energy Physics, Valencia, Spain, 2014 (unpublished) and references therein.
[53] M. Blanke, G. F. Giudice, P. Paradisi, G. Perez, and J. Zupan, J. High Energy Phys. 06 (2013) 022.
[54] S. Dawson *et al.*, arXiv:1310.8361.
[55] S. Heinemeyer *et al.* (LHC Higgs Cross Section Working Group Collaboration), arXiv:1307.1347.
[56] L. G. Almeida, S. J. Lee, S. Pokorski, and J. D. Wells, Phys. Rev. D **89**, 033006 (2014).
[57] G. P. Lepage, P. B. Mackenzie, and M. E. Peskin, arXiv: 1404.0319.
[58] H. Yokoya, Linear Collider Workshop2014, Belgrade, Serbia, 2014 (unpublished).
[59] C. Roda, 37th International Conference on High Energy Physics, Valencia, Spain, 2014 (unpublished).
[60] D. M. Asner *et al.*, arXiv:1310.0763.
[61] J. Tian and K. Fujii, *Proc. Sci.*, EPS-HEP2013 (2013) 316.
[62] P. Z. Skands *et al.*, J. High Energy Phys. 07 (2004) 036.
[63] A. Denner, Fortschr. Phys. **41**, 307 (1993).
[64] J. P. Lees *et al.* (*BABAR* Collaboration), Phys. Rev. Lett. **109**, 101802 (2012).
[65] J. P. Lees *et al.* (*BABAR* Collaboration), Phys. Rev. D **88**, 072012 (2013).
[66] J. Hasenbusch, 37th International Conference on High Energy Physics, Valencia, Spain, 2014 (unpublished).
[67] A. Crivellin, C. Greub, and A. Kokulu, Phys. Rev. D **86**, 054014 (2012).
[68] A. Crivellin, J. Rosiek, P. H. Chankowski, A. Dedes, S. Jaeger, and P. Tanedo, Comput. Phys. Commun. **184**, 1004 (2013).
[69] U. Nierste, S. Trine, and S. Westhoff, Phys. Rev. D **78**, 015006 (2008).
[70] A. Dedes, M. Paraskevas, J. Rosiek, K. Suxho, and K. Tamvakis, arXiv:1409.6546.
[71] A. Parker, *Proc. Sci.*, (ICHEP2012) (2012) 029.
[72] M. Backes, *Proc. Sci.*, (ICHEP2012) (2012) 105.
[73] G. Aad *et al.* (ATLAS Collaboration), Phys. Rev. D **87**, 012008 (2013).
[74] G. Aad *et al.* (ATLAS Collaboration), Phys. Rev. D **86**, 092002 (2012).
[75] G. Aad *et al.* (ATLAS Collaboration), ATLAS-CONF-2012-103.
[76] G. Aad *et al.* (ATLAS Collaboration), J. High Energy Phys. 07 (2012) 167.
[77] S. Chatrchyan *et al.* (CMS Collaboration), http://cdsweb.cern.ch/record/1460434.
[78] S. Chatrchyan *et al.* (CMS Collaboration), http://cdsweb.cern.ch/record/1460433.
[79] S. Chatrchyan *et al.* (CMS Collaboration), Phys. Rev. D **86**, 072010 (2012).
[80] S. Chatrchyan *et al.* (CMS Collaboration), Phys. Rev. Lett. **109**, 071803 (2012).
[81] S. Chatrchyan *et al.* (CMS Collaboration), Phys. Lett. B **716**, 260 (2012).
[82] A. Cakir (CMS Collaboration), *Proc. Sci.*, ICHEP2012 (2013) 126.
[83] G. Aad *et al.* (ATLAS Collaboration), Phys. Lett. B **720**, 13 (2013).
[84] G. Aad *et al.* (ATLAS Collaboration), Eur. Phys. J. C **72**, 2237 (2012).
[85] G. Aad *et al.* (ATLAS Collaboration), Phys. Rev. Lett. **109**, 211803 (2012).
[86] G. Aad *et al.* (ATLAS Collaboration), Phys. Rev. Lett. **109**, 211802 (2012).
[87] G. Aad *et al.* (ATLAS Collaboration), Eur. Phys. J. C **72**, 2174 (2012).
[88] G. Aad *et al.* (ATLAS Collaboration), Phys. Rev. D **85**, 112006 (2012).
[89] G. Aad *et al.* (ATLAS Collaboration), Phys. Rev. Lett. **108**, 241802 (2012).
[90] G. Aad *et al.* (ATLAS Collaboration), Phys. Rev. Lett. **108**, 181802 (2012).
[91] S. Chatrchyan *et al.* (CMS Collaboration), Phys. Rev. D **88**, 052017 (2013).
[92] S. Chatrchyan *et al.* (CMS Collaboration), Eur. Phys. J. C **73**, 2568 (2013).
[93] G. Aad *et al.* (ATLAS Collaboration), Phys. Lett. B **718**, 841 (2013).
[94] S. Chatrchyan *et al.* (CMS Collaboration), J. High Energy Phys. 11 (2012) 147.
[95] S. Chatrchyan *et al.* (CMS Collaboration), Phys. Lett. B **713**, 68 (2012).
[96] G. Altarelli, R. Barbieri, and F. Caravaglios, Int. J. Mod. Phys. A **13**, 1031 (1998).
[97] J. A. Casas and S. Dimopoulos, Phys. Lett. B **387**, 107 (1996).
[98] Y. K. Kim, 37th International Conference on High Energy Physics, Valencia, Spain, 2014 (unpublished).